SOCAR Proceedings

Reservoir Engineering

journal home page: http://proceedings.socar.az

HYDRODYNAMIC MODELING OF WATER–GAS INJECTION EFFECTS IN PERMEABILITY-HETEROGENEOUS RESERVOIRS

A. A. Aliyev[1], G. I. Jalalov[2], E. N. Mamalov*[2]

[1]*BP Azerbaijan, Baku, Azerbaijan*

[2]*The Azerbaijan National Academy of Sciences, Baku, Azerbaijan*

A B S T R A C T

In oil fields operated under depletion drive, improving oil recovery remains a critical challenge, requiring methods that can modify the physicochemical properties of the reservoir system, improve displacement efficiency, and provide additional pressure support. This study evaluates water-gas mixture (WGM) injection, supported by digital reservoir monitoring and numerical modeling, as an integrated approach for increasing the recovery of remaining oil reserves from heterogeneous reservoirs. A series of laboratory experiments was conducted using a linear reservoir model to compare the displacement efficiency of conventional waterflooding, WGM injection, and polyacrylamide (PAM) injection. The experiments show that WGM injection, particularly when applied from the early stage of development and compared with PAM-based mobility-control displacement, enables the target recovery factor to be achieved considerably faster. This improves the time-dependent oil recovery factor, shortens the overall development period, and reduces the required volume of the displacement agent. To validate the experimental conclusions under field-scale conditions, a hydrodynamic reservoir simulation study was performed for a selected block of the Gum Deniz oil field in Azerbaijan, which is characterized by complex geology, layered heterogeneity, and variable displacement behavior. The simulation workflow was implemented using the Landmark Nexus (Nexus-Black-Oil) software package and calibrated against historical production and pressure trends. The combined laboratory and numerical modeling results confirm that WGM injection can provide stronger pressure maintenance, improved sweep efficiency, and higher recovery potential than conventional waterflooding and PAM injection, making it a promising enhanced oil recovery strategy for mature depletion-drive reservoirs.

Keywords: enhanced oil recovery; water–gas mixture injection; sweep efficiency; oil displacement; heterogeneous reservoirs; history matching; polyacrylamide; PAM; EOR.

Date submitted: 14.02.2026 **Date accepted:** 30.04.2026

Introduction

Technological progress depends on its energy capacity. In turn, energy capacity, among other factors, depends on the oil production industry. To maintain stable oil production, it is necessary not only to discover new fields but also to enhance recovery from fields already under development. To intensify oil production, various reservoir stimulation and EOR methods are proposed and applied. Numerous studies by domestic and international authors have addressed different methods for enhancing oil recovery [1-14]. In particular, a significant amount of research conducted by Azerbaijani scientists and published in specialized journals such as SOCAR Proceedings and ANAS has explored the injection of water-gas mixtures (WGM), oil displacement mechanisms, and enhanced oil recovery in heterogeneous reservoirs. [1, 15, 16]. These studies provide foundational insights into the regional application of these methods.

To implement any technology under field conditions, its effectiveness must first be determined. The authors of this work conducted multiple laboratory experiments using PAM slug injection, WGM injection, and combinations of these approaches. The purpose of this paper is to identify the most effective of the two main methods listed above (PAM vs. WGM) to recommend it for field application.

Results of experiments and discussion

To perform a comparative analysis between experimental data obtained on a reservoir model and an actual reservoir, similarity conditions between the model and the prototype must be satisfied. Similarity may include hydrodynamic, geometric, physicochemical, and other aspects. Laboratory reservoir models differ significantly from real reservoirs in geometry, dimensions, porous medium, and other properties; therefore, approximate similarity is typically applied in laboratory practice.

This condition implies equality of the dimensionless groups (criteria) characterizing the displacement process

**E-mail:* evgeniy_mamalov@rambler.ru

http://dx.doi.org/10.5510/OGP20260201198

in both the model and the prototype. Although numerous similarity criteria exist, for oil displacement it is sufficient to ensure equality of the following dimensionless similarity criteria, Π_1 and Π_2 [8-10, 16-21].

Criteria Π_1

Criterion Π_1 characterizes the structure of the porous medium. The dimensionless length of the reservoir model accounts for the influence of reservoir size and porous-medium properties on displacement performance and is defined as follows:

$$\Pi_1 = \frac{L}{\sqrt{k}} \quad (1)$$

where L is reservoir length (m), and k is permeability (μm²).

Criteria Π_2

Criterion Π_2 reflects the influence of hydrodynamic forces on phase distribution within pores and is equal to the ratio of the capillary-force gradient to the macroscopic pressure drop in the reservoir. It is determined by:

$$\Pi_2 = \frac{P_c}{\Delta P} = \frac{\sigma \cdot \cos\theta}{\Delta P \cdot \sqrt{\frac{k \cdot \varphi}{m}}} \quad (2)$$

where P_c is capillary pressure at the oil–displacing agent interface, ΔP is the pressure drop in the reservoir (MPa), σ is interfacial tension at the oil–water interface (mN/m), θ is the contact angle, φ is a structural coefficient, and m is porosity. For a layered heterogeneous reservoir, values of k and m are taken from the low-permeability layer.

It is not possible to satisfy Π_1 and Π_2 simultaneously. However, as shown in [8, 17-19], exact matching of these criteria is not strictly required for modeling. There are ranges in which variations in these criteria have a minor effect on oil recovery, corresponding to the onset of self-similarity (automodel behavior). Calculations showed that the model dimensions and experimental procedure satisfy the following conditions:

$$\Pi_1 \geq 0.5 \times 10^6 \quad \text{and} \quad \Pi_2 \leq 0.6 \quad (3)$$

In addition, the correctness of the model selection is evaluated using the minimum reservoir length:

$$L_{\min} = \frac{\Pi_1}{\Pi_2} \cdot \sqrt{km} \quad (4)$$

Therefore, the results can be transferred to a real oil reservoir. Accordingly, the experimental reservoir model was verified against the aforementioned similarity criteria. The calculations confirmed that the model parameters and the filtration–capacity properties of the porous medium meet the similarity requirements.

Reservoir model and experimental setup

The homogeneous linear reservoir model had the following initial parameters: length 84 cm and diameter 25 mm. The model volume was 412.44 cm³. The porous medium consisted of a mixture of quartz sand with fractions of 0.2–0.125 mm and sand with a fraction of less than 0.125 mm.

In the experiments, oil sampled from well No. 1289 of the PK horizon of the Palchiq Vulkani field was used. The oil viscosity at 20–25 °C was 205 mPa·s, and the density was 922 kg/m³. The paraffin content was 0.42%, sulfur – 0.20-0.22 %, silica-gel resins – 12-14 %, and asphaltenes – 1.4%.

To achieve the stated objective, experiments were conducted to displace oil from the porous medium by injecting PAM solutions of different concentrations, as well as WGM. The displacement using the investigated methods was applied from the very beginning of the process.

For the PAM injection cases, it was assumed that PAM affects only the viscosity of the injected water, with zero adsorption and no impact on the properties of the WGM.

The main results are presented in table 1.

Comparison of three displacement modes

For clearer interpretation, three displacement modes were considered:

- Depletion-like mode: oil is displaced by injecting distilled water.
- PAM flooding mode: oil is displaced by a PAM solution slug.
- WGM mode: oil is displaced by a water–gas (water–air) mixture.

As shown in table 1, the initial conditions are approximately the same across all experiments, enabling direct comparison of results. In Experiment 1, oil displacement was performed with distilled water. In Experiments 2 and 4, oil was displaced using PAM solutions with concentrations of 0.1 and 0.2 %, respectively. The mechanism of PAM solution action is based on water thickening (i.e., increasing its viscosity). The higher PAM concentration corresponds to higher solution viscosity (figs. 1-3).

In Experiment 3, oil was displaced by a WGM. The mechanism of WGM is associated with changes in mixture properties and a reduction in oil viscosity; the combination of these effects enhances oil recovery from the reservoir.

Table 1

Key experimental results

Parameter	Experiment 1	Experiment 2	Experiment 3	Experiment 4
Oil viscosity at 25°C, mPa·s	205	205	205	205
Permeability to air, μm²	0.60	0.59	0.63	0.64
Permeability to water, μm²	0.52	0.54	0.55	0.50
Initial oil saturation, %	74.4	74.3	75.8	74.7
Pore volume of the model, cm³	170	164	163	162
Injected water volume, pore volumes	2.5	–	4.4	–
Injected air volume, pore volumes	–	–	194.8	–
Water–air ratio, cm³/cm³	–	–	0.0226	–
PAM concentration, %	–	0.1	–	0.2
PAM volume, pore volumes	–	1.88	–	2.86
PAM viscosity, mPa·s	–	12	–	27
RF, %	31.0	54.5	60.0	59.5
Pressure drop, MPa	0.5	0.5 and 0.9	0.35–0.52	0.5 and 0.8

Effective viscosity of WGM in porous media

In addition to the intrinsic properties of PAM, oil displacement and the propagation of the injected slug may be influenced by a water–gas emulsion formed within the porous medium, whose viscosity is higher than the viscosity of water and gas separately. The viscosity of the WGM under reservoir conditions can be estimated using the Einstein relation [6, 15, 22]:

$$\mu_{mix} = \mu 0\left(1 + 2.4R_c\right) \quad (5)$$

where μ_0 is water viscosity (mPa·s), and R_c is the volumetric fraction of gas in the WGM under reservoir conditions (m^3/m^3), defined as:

$$R_c = \frac{V_{g.res}}{V_{g.res} + V_{w.inj}} \quad (6)$$

where $V_{g,res}$ is the injected air volume under reservoir conditions (m^3) and $V_{w,inj}$ is the injected water volume (m^3). During the experiments, the ambient temperature was 25–27 °C; therefore, water viscosity was taken as μ_0=0.8937 mPa·s.

The viscosity of the WGM under reservoir conditions increases directly with the gas fraction in the mixture. The average viscosity of the WGM was approximately 2.5 mPa·s. By varying the water-to-gas ratio, the amount of oil displaced can be controlled.

WGM behavior and comparison with PAM flooding

Considering water–gas displacement in more detail, the WGM stabilizes at approximately $\tau \approx 0.2$. During this period, a sharp increase in WGM parameters is observed, accompanied by intense oil displacement. After transitioning to a constant (stable) water–gas ratio, the oil RF grows more slowly and approaches stabilization (fig. 4).

The next step is to compare the WGM and PAM flooding in terms of potential interchangeability. While RF differs between displacement methods, by varying the PAM concentration it is possible to reach the same RF as with the WGM. With nearly identical initial data, the oil RF is about 60%. However, PAM flooding significantly extends the process duration.

Achieving a similar oil RF with PAM solution injection requires an experiment duration approximately four times longer than that required for WGM. Furthermore, a comprehensive comparison between WGM and PAM must consider the theoretical and practical limitations of chemical agents. Unlike WGM, the application of PAM involves significant operational risks, including PAM adsorption, mechanical and chemical degradation, retention within the porous medium, reduced injectivity, and potential formation damage. These factors demonstrate that the superiority of WGM is justified not only by accelerated oil recovery but also by a reduction in the operational risks commonly associated with chemical agents. However, for a final field-scale selection, additional site-specific laboratory and pilot data will be essential.

In addition, the cost of the components for each method must be considered. Thus, the experiments demonstrate that injecting WGM is more economical both in terms of process duration and overall cost. However, while the technical screening demonstrates significant advantages of WGM injection in terms of process duration, it is important to recognize that this study represents an initial technical evaluation rather than a comprehensive field-scale economic model.

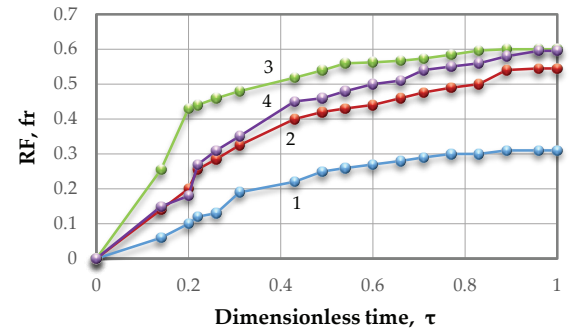

1-oil displacement by distilled water
2-oil displacement by a 0.1% PAM
3-oil displacement by a WGM
4-oil displacement by a 0.2% PAM

$\tau = ti / \sum ti$ where ti is the current time (hr) and $\sum ti$ is the total duration of the experiment

Fig. 1. Dependence of the oil RF on dimensionless time

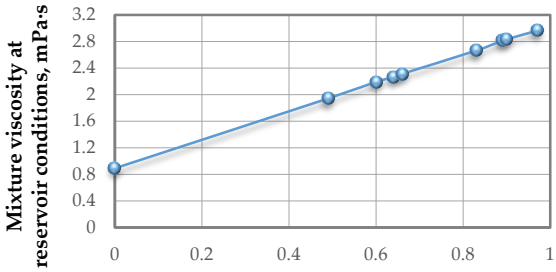

Fig. 2. Dependence of mixture viscosity on the volumetric fraction of air in the mixture under reservoir conditions

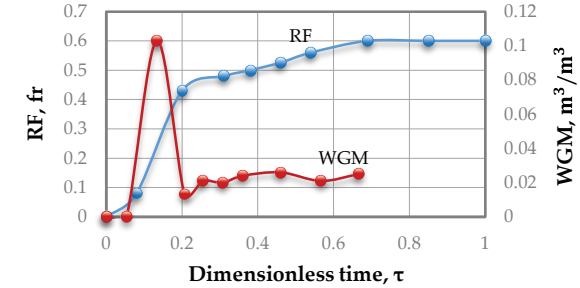

Fig. 3. Dependence of the RF and WGM on dimensionless time

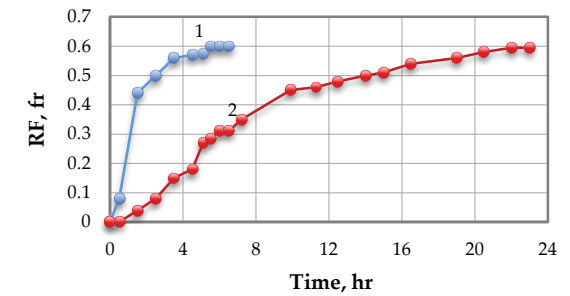

1 – oil displacement by WGM (Experiment No. 3)
2 – oil displacement by 0.2% PAM solution (Experiment No. 4)

Fig. 4. Comparison of RF progression for WGM and PAM4

The ultimate economic efficiency and industrial viability of WGM implementation will heavily depend on specific infrastructure scenarios, including the availability of a reliable gas source, gas preparation and compression facilities, capital expenditures (CAPEX) for surface equipment, and ongoing operational expenditures (OPEX). A full economic justification integrating these infrastructure constraints is required before commercial application.

Evaluating WGM injection impact on real oil field

Using the software suite from the company Landmark, Nexus-Black Oil simulator, the application of the WGM method was investigated for a pilot area of the Gum Deniz field.

In addition, a hydrodynamic model was constructed and history-matched to the actual production history.

Figure 5 shows a geometric representation of a block from the Gum Deniz field. A block located in the northwestern area of the field was chosen, and three primary productive layers, namely Fasila reservoir (FLD1, FLD2, and FLD3 subzones)— were selected to be evaluated. The entire analysis is based on physical data for these horizons, as well as on wells completed in these zones.

As in many mature oil fields, similar trends observed at the Gum Deniz field necessitate the application of EOR methods to maximize the recovery of additional hydrocarbon reserves. In the oil and gas industry, this objective is commonly addressed through a range of technological approaches, including conventional water injection, gas injections, and chemical injections. In recent years, WGM has attracted particular attention. This technology involves injecting water with increased effective viscosity into the reservoir and is regarded as a promising option for improving sweep efficiency, reducing early water breakthrough, and ultimately enhancing oil recovery. It should be emphasized that the term 'viscosity-enhanced waterflooding' provides only a simplified description of the WGM process. Terminologically and physically, the impact of WGM is not limited strictly to an increase in the effective viscosity of the injected water. It is a multi-factor mechanism that also encompasses the improvement of the mobility ratio, reduction in the apparent viscosity of the oil, and modification in capillary forces and interfacial interactions within the porous medium.

The objective of this paper is to evaluate the technological performance and potential economic benefits of implementing WGM water injection in the Gum Deniz oil field. Within the scope of the study, the impact of WGM injection on production rates, ultimate oil recovery, and water-cut dynamics is analyzed, taking into account the reservoir heterogeneity. The study aims to more clearly demonstrate the applicability of WGM injection as an EOR method for highly water-cut, mature oil fields.

For a selected block within the Fasila reservoir interval, a hydrodynamic model was constructed based on the existing geological model, with integration of actual well production measurements. This block was selected as it represents one of the key development areas of the field, exhibiting significant remaining oil potential and active production behavior. In addition, the oil–water contact (OWC) in this area is relatively well constrained, supported by both well log interpretation

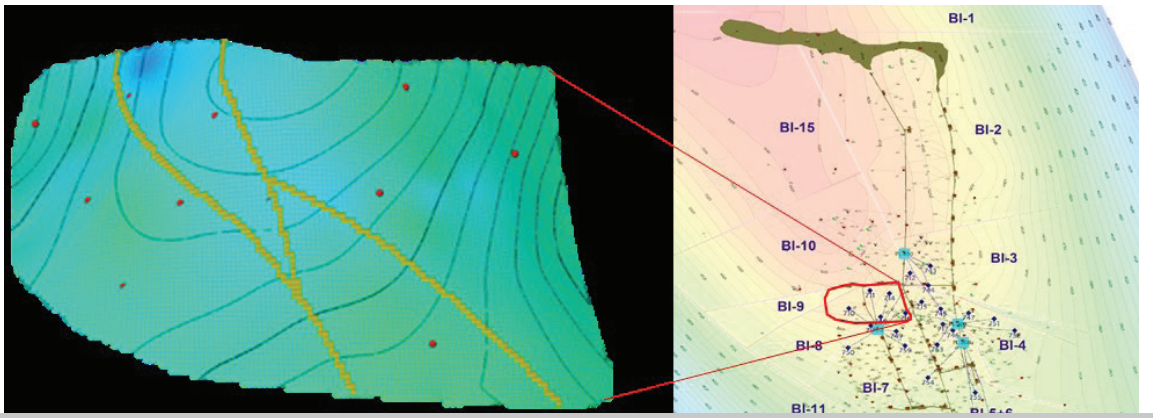

Fig. 5. Selected block for analysis

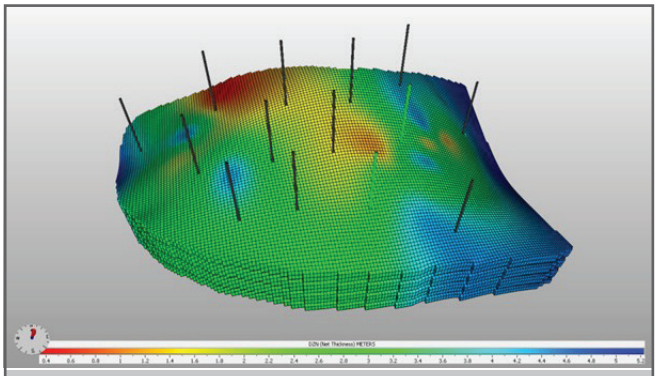

Fig. 6. Effective net thickness map

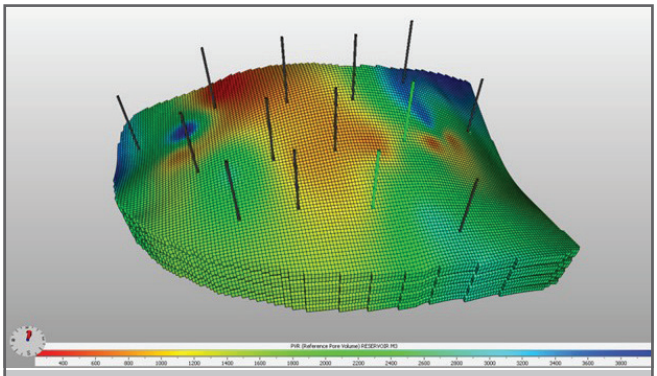

Fig. 7. Pore volume distribution map

and pressure transient analysis (PTA) results, which reduces structural and fluid uncertainties. The availability of reliable dynamic and static data makes this block particularly suitable for detailed modeling and development studies. For the selected block within the Fasila reservoir interval, the simulation model was built on a Cartesian grid, corresponding to 781,200 active grid cells, with a uniform cell size of .

The model was subsequently calibrated through history matching. The main objective was to develop a reliable hydrodynamic model capable of reproducing historical field performance and, thereafter, to use this model for forecasting in order to accurately assess EOR options and perform their comparative evaluation.

Based on well log data, the average reservoir properties for the Fasila interval are approximately: porosity 0.23, initial water saturation 0.30, net-to-gross ratio 0.55, and permeability approximately 110 mD (table 2, figs. 3–7).

The black-oil PVT was generated in the Nexus model using standard black-oil correlation methods. The base PVT trends were initially established based on an analogue field dataset, together with legacy Gum Deniz rock-fluid information and historical core-supported data available for the Fasila interval. These initial correlations were subsequently calibrated to match the available measured PVT and production-surveillance data, the most important of which include bubble-point pressure and viscosity behavior, to ensure that the simulated fluid response remains consistent with actual reservoir performance under current operating conditions. The use of historical rock and fluid datasets for characterizing Gum Deniz field is also discussed by Gumrah et al. (2012), providing supporting constraints for reservoir descriptions based on legacy information [3, 4].

The heavy-oil viscosity used in the laboratory (≈205 cP at 25°C) serves as a screening condition to accentuate mobility-control effects, whereas the Gum Deniz model applies the actual reservoir-consistent viscosity (≈4–6 cP), so the lab–field viscosity mismatch is not a limitation for evaluating method ranking and expected recovery trends (fig. 8).

Table 2

Key experimental results

Parameter	Symbol	Average / Range	Unit	Notes
Porosity	φ	0.22–0.24	fraction	Based on log interpretation and model distribution
Net-to-Gross	NTG	0.55–0.60	fraction	Effective sand fraction
Horizontal permeability	K_h	90–120	mD	Average from geological model
Vertical permeability	K_v	10–20	mD	Anisotropy considered
Permeability ratio	K_v/K_h	0.01-0.10	fraction	Layered heterogeneity
Effective reservoir thickness	H_{eff}	10–14	m	Selected block
Initial reservoir pressure	P_i	~140-160	bar	From history-matching results
Initial oil saturation	S_{oi}	0.65–0.70	fraction	Model initial condition
Initial water saturation	S_{wi}	0.30–0.35	fraction	Capillary effects not considered
Oil viscosity at reservoir conditions	μ_o	4–6	cP	PVT matching
Water viscosity	μ_w	0.45	cP	Standard water injection
WGM viscosity	μ_w	2.5	mPa·s (≈cP)	Used to represent the WGM effect
Oil formation volume factor	B_o	1.20–1.30	m³/m³	Based on PVT data

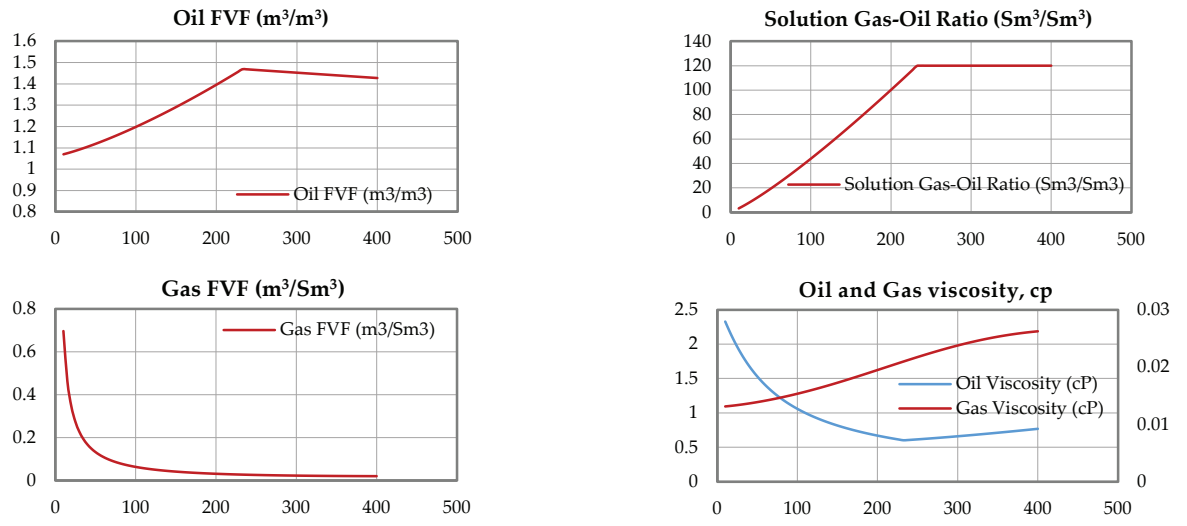

Fig. 8. PVT plots

History matching

In the hydrodynamic model, measured field production data (oil, gas, and water) were compiled for all existing producing wells completed in the Fasila reservoir interval. Where direct phase-rate measurements were not available, the produced water fraction was estimated from wellhead fluid samples, and oil rates were allocated accordingly. These time-series datasets were used as the primary inputs for model calibration (history matching).

During the history-matching process, limited reservoir pressure information was also utilized. Both directly measured reservoir pressures (e.g., from shut-in surveys) and pressures estimated from bottomhole and/or wellhead measurements were treated as observed data and integrated into the calibration workflow.

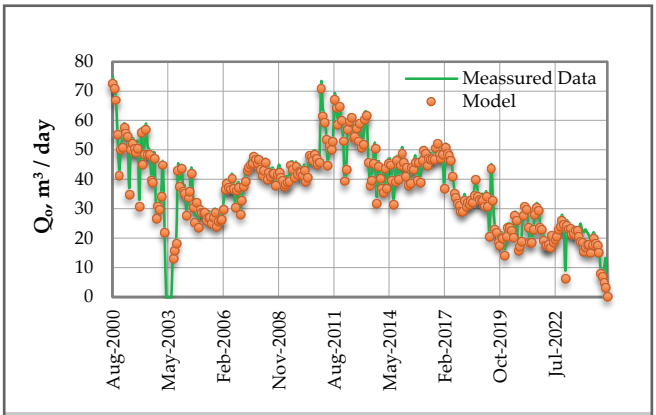

Fig. 9. Oil rate history match

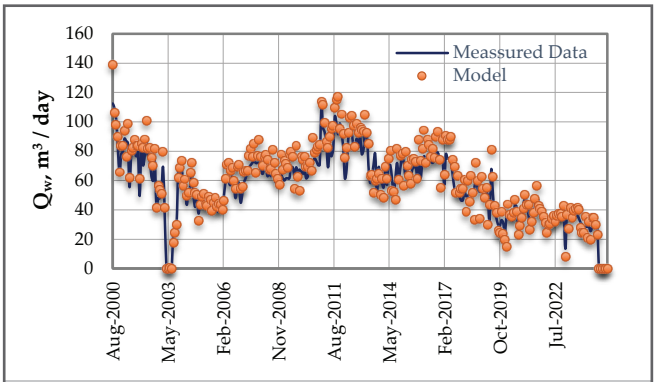

Fig. 10. Water rate history match

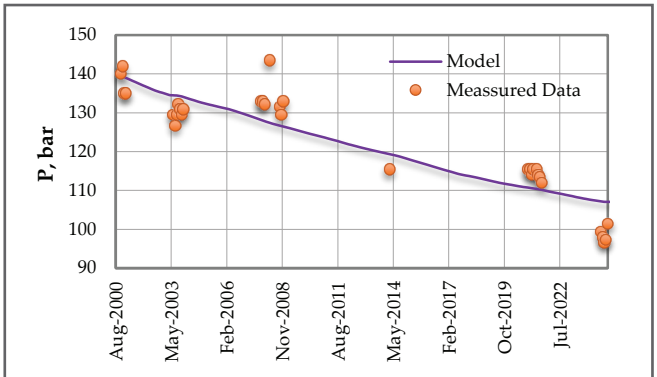

Fig. 11. Average reservoir pressure match

History matching was performed primarily on the combined oil and water (total liquid) response, rather than simultaneously matching oil, gas, and water rates. This choice reflects the higher uncertainty typically associated with gas-rate measurement and allocation, and the fact that produced gas is often dominated by solution-gas behavior (i.e., GOR-driven response) and operational effects. In contrast, liquid rate and water cut generally provide a more robust and consistent indication of reservoir performance and water movement and therefore were prioritized for calibration. Gas trends were still reviewed as a secondary check to ensure overall consistency.

Multiple history-matching scenarios were evaluated by varying: (i) relative permeability curves and their endpoint parameters, (ii) original oil in place (OOIP), (iii) aquifer strength, and (iv) transmissibility parameters controlling flow across geological faults. Hydrodynamic model calibration is based on minimizing the mismatch between observed and model-predicted responses [1, 3, 15]. To this end, mismatches in reservoir pressure, oil production, and water production were combined into a single objective function [16]:

$$J(\theta)=\sum_{i=1}^{N_w}\sum_{t=1}^{T}\left[w_P\left(\frac{P_{i,t}^{model}(\theta)-P_{i,t}^{obs}}{\sigma_{P,i}}\right)^2+\right.$$
$$\left.+W_o\left(\frac{q_{o,i,t}^{model}(\theta)-q_{o,i,t}^{obs}}{\sigma_{o,i}}\right)^2+W_w\left(\frac{q_{w,i,t}^{model}(\theta)-q_{w,i,t}^{obs}}{\sigma_{w,i}}\right)^2\right]$$

where $J(\theta)$ – objective (misfit) function that quantifies the overall mismatch between observed (field) data and model predictions and is minimized during history matching; θ – vector of adjustable (calibration) model parameters (e.g., relative permeability curve parameters, aquifer strength, inter-fault transmissibility, original hydrocarbons in place, etc.); $P_{i,t}^{model}$, $P_{i,t}^{obs}$ – model-predicted and measured bottomhole pressure for well (i) at time step (t), respectively; $q_{o,i,t}^{model}$, $q_{o,i,t}^{obs}$ – model-predicted and observed oil production rate for well (i) at time step (t), respectively; $q_{w,i,t}^{model}$, $q_{w,i,t}^{obs}$ – model-predicted and observed water production rate for well (i) at time step (t), respectively; $\sigma_{p,i}$, $\sigma_{o,i}$, $\sigma_{w,i}$ – standard deviations representing measurement uncertainty in pressure, oil-rate, and water-rate observations, respectively. These parameters control the relative penalty of deviations in the misfit function: a smaller σ results in a larger contribution (higher penalty) to the misfit, while a larger σ reduces the contribution (lower penalty); W_P, W_o, W_w – weighting factors that reflect the reliability of different data types and their relative importance in the optimization (history-matching) process.

It should be noted that, within the scope of this study, the minimization of the objective function was not carried out directly using explicit mathematical optimization algorithms. The hydrodynamic model was calibrated using the Landmark Nexus Reservoir Simulator, and the matching process was primarily based on a visual comparison of production and pressure trends. Nevertheless, from a mathematical standpoint, the history-matching procedure can still be formulated as minimizing the mismatch between observed field data and model-predicted responses, which is equivalent to the objective function presented in this work.

In other words, although history matching can formally be expressed as an objective-function minimization problem, in practical application the minimization was achieved iteratively through the simulator's internal mechanisms and

engineering judgment. This approach preserved the physical consistency of the model while enabling a reliable reproduction of historical field performance (figs. 9-11).

Relative permeability and model calibration (history matching)

Determination of relative permeability curves is typically performed in high-technology laboratories through special core analysis (SCAL) using core samples. However, because SCAL programs are often costly and time-consuming, relative permeability data are frequently adopted from analogue reservoirs or estimated using Corey-type correlations and subsequently refined during the history-matching process. For the Gum Deniz field, SCAL data were not available; therefore, at the initial stage the model was populated with relative permeability curves generated using the standard Corey functional form [2]:

$$k_{rw} = k_{rw}^{0} \times \left(S_w^*\right)^{n_w}$$

$$k_{ro} = k_{ro}^{0} \times \left(S_w^*\right)^{n_o}$$

where k_{rw}^{0} – endpoint relative permeability to water; k_{ro}^{0} – endpoint relative permeability to oil; n_w, n_o – Corey exponents for water and oil, respectively

During hydrodynamic model calibration, relative permeability was treated as one of the key history-matching parameters. The analysis was performed using two model variants: (i) a base case built with initial (unmatched) relative permeability curves and (ii) a calibrated case using history-matched relative permeability curves. In the initial variant, the relative permeability functions were generated using a standard Corey formulation for the reservoir rock and were adjusted only to be consistent with the limited well-level information available.

At the history-matching stage, both the shape of the relative permeability curves and their endpoint parameters were adjusted to reproduce the observed production behavior. In this process, measured and simulated oil and water production responses were compared, with particular focus on water breakthrough timing, water-cut growth rate, and oil-rate decline trends as the primary matching criteria. Calibration of relative permeability enabled the model to more accurately represent the actual water–oil flow behavior within the reservoir.

It should be noted that relative permeability is not a parameter that can be measured directly at the reservoir scale; therefore, its estimation is typically performed indirectly through production data matching. In this context, the history-matched relative permeability curves represent not only near-wellbore flow behavior but also the effective hydrodynamic behavior of the reservoir in the interwell region.

Overall, the calibration of relative permeability played a central role in improving model reliability and enabled a realistic reproduction of dynamic production, particularly the water-cut evolution and the oil-rate decline trends (figs.12, 13).

Impact of waterflooding on oil production

To evaluate the impact of waterflooding in a more objective and comparative manner, forecast simulations were performed for the selected block. Within this framework, 19 new producing wells and 5 new water injection wells were drilled and brought onstream in a phased manner at different times, and the long-term production behavior was analyzed. The constructed scenarios enabled a direct comparison between cases with no waterflooding, conventional waterflooding, and viscosity-enhanced waterflooding.

For modeling WGM water injection, the effect was represented in the Nexus black-oil simulator by assigning an increased water viscosity of μ_{mix}=2.5 mPa·s, thereby providing a simplified proxy for the WGM behavior. This representation was intentionally simplified within the framework of a black-oil approach. It is acknowledged that this proxy method does not fully capture complex physical phenomena such as dynamic gas distribution within the reservoir, local mixing dynamics, phase behavior, and possible inter-phase capillary effects. However, the primary goal of this study was to verify the feasibility of representing this complex physical process with acceptable accuracy and minimal error using a computationally practical model to evaluate sweep efficiency and mobility control. While gas metrics were used only as secondary checks during the history matching process, future research will require the development of more advanced multi-phase or fully compositional chemical simulation model to capture the complete mathematical and physical interactions of the gas phase.

It should be noted that WGM injection can also be

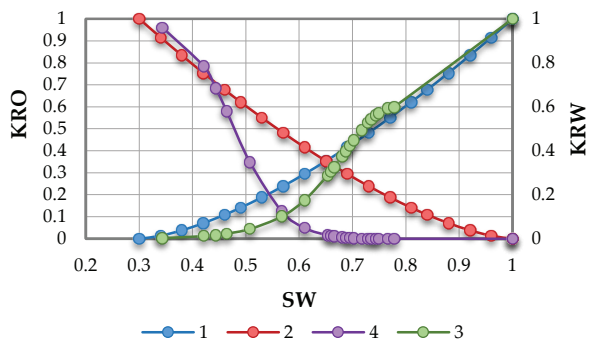

1 – Oil relative permeability before history matching
2 – Water relative permeability before history matching
3 – Oil relative permeability after history matching
4 – Water relative permeability after history matching

Fig. 12. Water-oil relative permeabilities

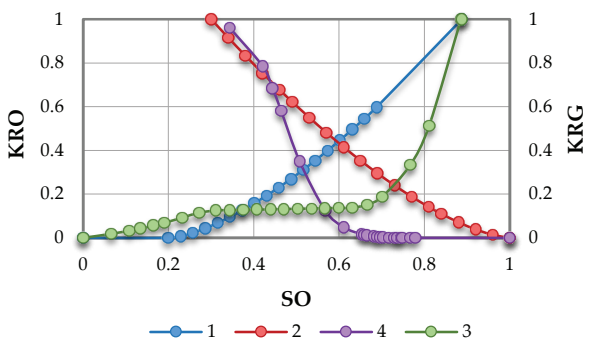

1 – Oil relative permeability before history matching
2 – Gas relative permeability before history matching
3 – Oil relative permeability after history matching
4 – Gas relative permeability after history matching

Fig. 13. Gas-oil relative permeabilities

described using more complex multicomponent chemical modeling approaches. However, based on preliminary assessments and the objectives of this study, it was concluded that such complexity would not materially change the conclusions, and a computationally efficient simplified approach was adopted. This methodology captures the key mechanism by modifying water mobility and improving sweep efficiency in a robust manner (figs.-14-18).

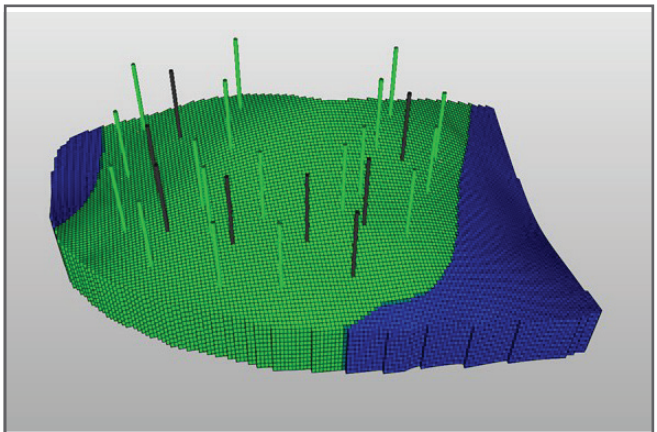

Fig. 14. New well locations-producer (green) and injector (dark blue)

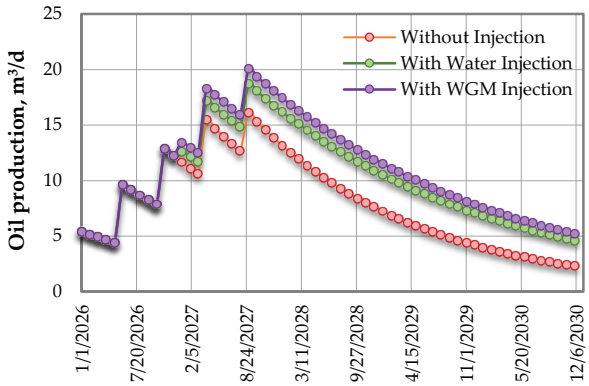

Fig. 15. Oil production prediction comparison

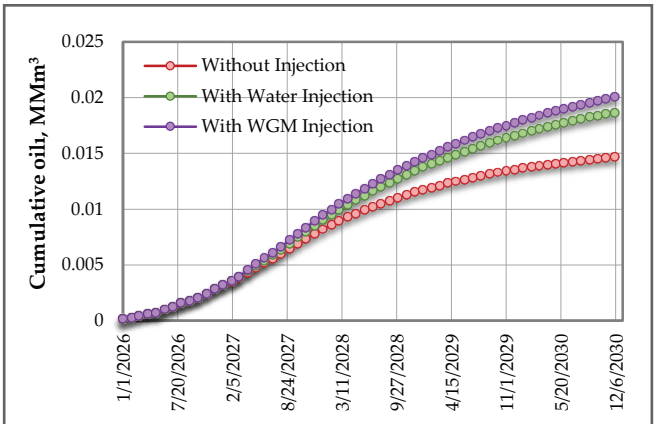

Fig. 16. Cumulative oil production prediction comparison

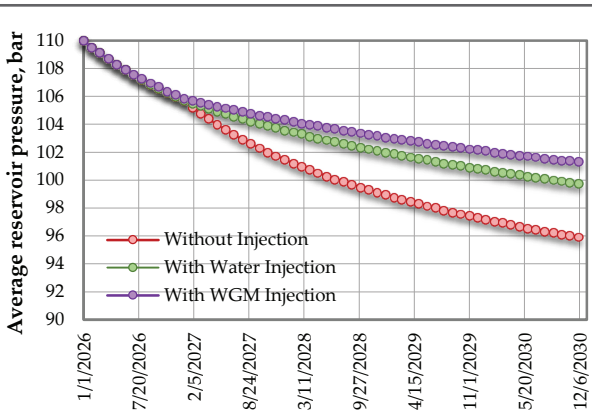

Fig. 17. Average reservoir pressure prediction comparison

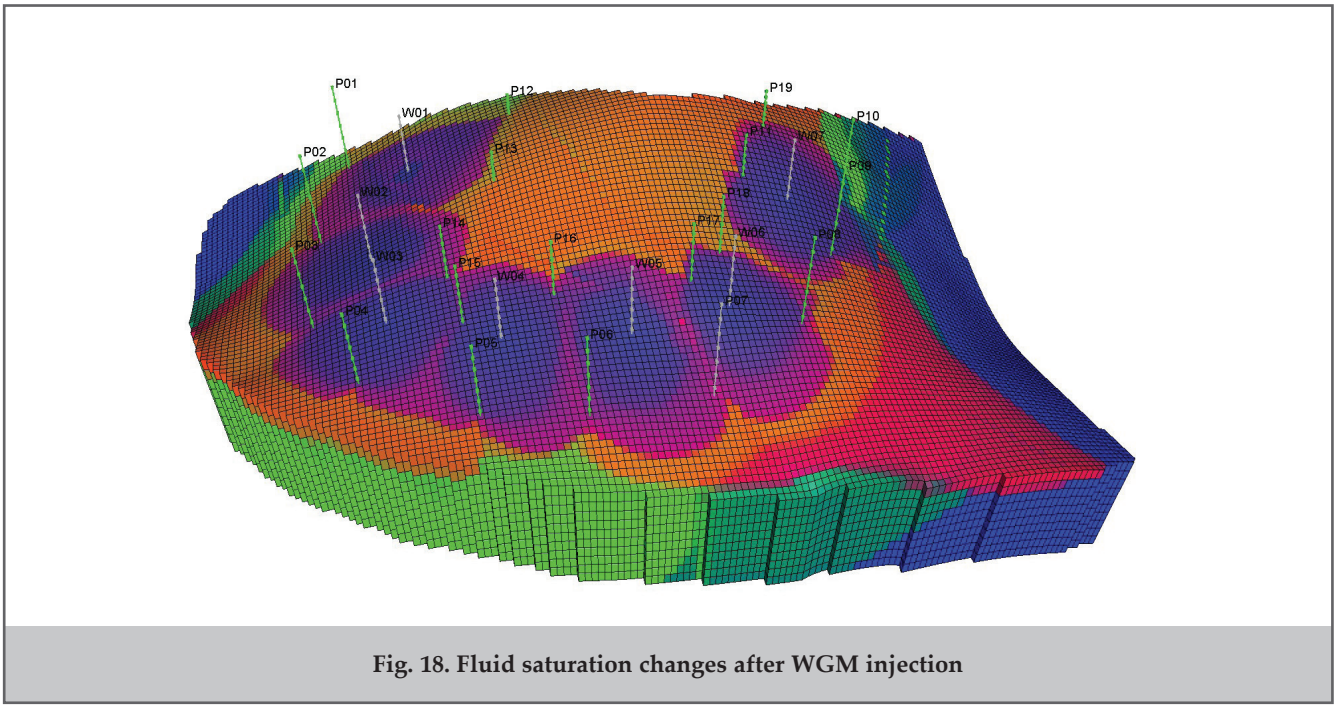

Fig. 18. Fluid saturation changes after WGM injection

Conclusions

- The hydrodynamic modeling and forecast simulations clearly demonstrate the impact of conventional waterflooding and viscosity-enhanced waterflooding on oil production from the Fasila interval of the Gum Deniz oil field. For comparison, results from three scenarios were analyzed in terms of oil rate, cumulative oil production, and reservoir pressure dynamics.
- In the first scenario (no waterflooding; production wells only), a rapid decline in reservoir pressure is observed. Although the early production period is characterized by relatively high rates, the sustained pressure depletion quickly leads to a sharp drop in oil rates. In this case, the rate of oil production decline is high, and cumulative oil production serves as the baseline level relative to the other scenarios. The results indicate that exploitation relying solely on natural reservoir energy is not an efficient long-term strategy for mature and highly water-cut reservoirs such as Gum Deniz.
- In the second scenario (conventional waterflooding), the rate of reservoir pressure decline is noticeably reduced. With pressure support, the oil-rate decline is lower than in the first scenario, and oil production is sustained for a longer period. In this case, cumulative oil production increases by approximately 27% compared with the no-waterflood baseline. However, due to reservoir heterogeneity, injected water preferentially flows through high-permeability zones, leading to early water breakthrough and limiting the overall effectiveness of the waterflood.
- The third scenario (viscosity-enhanced waterflooding) delivers the most favorable performance. Increasing water viscosity improves the water–oil mobility ratio, promotes a more uniform areal/vertical distribution of the injected fluid, and significantly expands sweep efficiency. The simulation results show that early water breakthrough is mitigated, lower-permeability zones of the reservoir are contacted more effectively, and the oil-rate decline is minimized. As a result, cumulative oil production is approximately 36% higher than the baseline scenario.
- Overall, the analysis indicates that under the heterogeneous reservoir conditions of the Gum Deniz field, conventional waterflooding alone provides limited incremental benefit. In contrast, viscosity-enhanced waterflooding demonstrates higher technological effectiveness by delivering a greater production increase and maintaining reservoir pressure more effectively, making it a more suitable approach for long-term development and improved oil recovery.

References

1. Abdullaev, V. D., Ibrahimov, Kh. M., Kyazimov, F. K., Shafiyev, T. Kh. (2016). Experimental studies on gas drive and gas-and-water oil displacement. *SOCAR Proceedings*, 1, 51-57.

2. Corey, A. T. (1954). The interrelation between gas and oil relative permeabilities. *Producers Monthly*, 19(1), 38–41.

3. Green, D. W., Willhite, G. P. (1998). Enhanced oil recovery. SPE Textbook Series, Vol. 6. *Society of Petroleum Engineers*.

4. Gumrah, F., Aliyev, A., Guliyeva, J., Ozavci, O. (2012). Determining reservoir characteristics and drive mechanisms for an oil reservoir. *SOCAR Proceedings*, 4, 22–31.

5. Gumrah, F., Aliyev, A., Ozavci, O. (2015). Evaluation of drive mechanisms on offshore oil reservoirs by analytical methods. Proceedings of ANAS. *The Sciences of Earth*, 3, 15–24.

6. Irani, M. M., Telkov, V. P. (2021). Study of modern options for using combinations of gas and traditional flooding (water-gas impact and its alternative). *SOCAR Proceedings*, 2, 248–256.

7. Kazimov, Sh. P. (2022). Enhanced oil recovery in water-flooded and hard-to-recover reservoirs. *SOCAR Proceedings*, 1, 89–93.

8. Mamalov, E. N., Gorshkova, E. V. (2025). Intensification of oil production using a combined method of influencing formations. *Baku: Ocaq.*

9. Mamalov, E. N., Jalalov, G. I., Gorshkova, E. V., Hadiyeva, A. S. (2022). Intensification of oil production using WGM. *SOCAR Proceedings*, 2, 78–83.

10. Suleimanov, B. A., Abbasov, H. F. (2022). Enhanced oil recovery mechanism with nanofluid injection. *SOCAR Proceedings*, 3, 28–37.

11. Suleimanov, B. A., Abbasov, H. F., Ismayilov, R. H. (2023). Enhanced oil recovery with nanofluid injection. *Petroleum Science and Technology*, 41(18), 1734–1751.

12. Suleimanov, B. A., Veliyev, E. F. (2016). Softened water application for enhanced oil recovery. *SOCAR Proceedings*, 2, 24-28.

13. Telkov, V. P., Mostadjeran, M. G. (2018). Evaluation of criteria for the application of polymer flooding for the displacement of heavy, highly viscous Iranian oils. *Oil Gas Exposure*, 4(64), 52-55.

14. Gasimli, A. M., Jamalov, I. M., Aliyev, N. Sh., Kazimov, F. K. (2008). On increasing oil recovery from reservoir layers with different permeabilities. *Azerbaijan Oil Industry*, 3, 36–39.

15. Jalalov, G. I., Aliyev, A. A. (2024). Study of unsteady state flow in a deformable formation under two-phase flow condition. *SOCAR Proceedings*, 2, 4–11.

16. Oliver, D. S., Chen, Y. (2011). Recent progress on reservoir history matching: a review. *Computational Geosciences*, 15(1), 185–221.

17. Efros, D. A., (1963). A study of the filtration of heterogeneous systems. *Moscow: Gostoptekhizdat.*

18. Lake, L. W. (1989). Enhanced oil recovery. *New Jersey: Prentice Hall, Englewood Cliffs.*

19. Mamalov, E. N., Gorshkova, E. V. (2020). One opportunity to increase oil recovery in a layered heterogeneous reservoir. *Azerbaijan Oil Industry*, 3, 20–26.

20. Manrique, E. J., Thomas, C. P., Ravikiran, R. (2010). EOR: current status and opportunities. *SPE Reservoir Evaluation & Engineering*, 13(06), 946–956.

21. Sheng, J. J. (2015). A comprehensive review of alkaline–surfactant–polymer flooding. *SPE Reservoir Evaluation & Engineering*, 18(03), 357–372.

22. Jalalov, G. I., Ibragimov, T. M., Aliyev, A. A., Gorshkova, E. V. (2018). Modeling and research of filtration processes in deep-seated oil and gas fields. *Baku: Elm ve Tehsil.*